Laser processing in 3D diamond detectors

DOI:
10.1016/j.nima.2016.04.052

Document Version
Accepted author manuscript

Laser Processing in 3D Diamond Detectors

S A Murphy[a,*], M Booth[b], L Li[c], A Oh[a], P Salter[b], B Sun[b], D Whitehead[c], A Zadoroshnyj[d]

[a] *School of Physics and Astronomy, The University of Manchester, UK*
[b] *Department of Engineering Science, The University of Oxford, UK*
[c] *School of Mechanical, Aerospace, and Civil Engineering, University of Manchester, UK*
[d] *School of Materials, University of Manchester, UK*

Abstract

A technique for electrode production within diamond using a femtosecond laser system is described. Diagnosis tests to quantify the stress, the diamond to graphite ratio, and the resistivity of these electrodes are discussed. A 3D electronic grade single crystal diamond detector produced using this technique is shown, and the electrodes have a resistivity of O(1 Ωcm). An improvement to the technique through the use of an adaptive wavefront shows a reduction of the diamond to graphite ratio, and smaller, higher quality electrodes were manufactured.

Keywords: 3D diamond detectors, Laser graphitisation of diamond, Single crystal diamond

1. Introduction

Tracking detectors are used to determine the position and momentum of charged particles in the ATLAS and CMS experiments, and these detectors currently use a silicon wafer. The detectors are subjected to high levels of radiation, which affects the properties of the silicon wafer. This reduces the detection efficiency, and the detector must be periodically replaced. Diamond is being considered as an alternative material to survive radiation levels of O(10^{16})

*Corresponding author
Email address: steven.murphy@manchester.ac.uk (S A Murphy)

particles per cm^2 due to its radiation hardness and lower noise. However the current electrode fabrication technique for diamond limits the diameter and resistivity of the electrodes to 6 µm and O(1 Ωcm) respectively.

In this paper the current fabrication technique of electrodes for a 3D diamond detector is discussed, and an improvement to this technique using a dynamically adaptive wavefront is demonstrated in Section 2. Detectors manufactured using the existing and the improved techniques are discussed in Section 3, showing a comparison of the electrical properties, the material content, and the induced stress of the electrodes.

2. Detector fabrication

The electrodes in diamond are fabricated using a Coherent Libra Ti-Sapphire femtosecond laser, operating in TEM_{00} beam mode with a wavelength of 800 nm and a 100 fs pulse duration [1]. This causes a phase transition from diamond to graphite at the focal point. Shorter pulse lengths produce more uniform structures, but with higher resistivity than longer (O(ps)) pulse lengths [2]. The electrodes are produced with this laser process [3], where the electrodes likely consists of amorphous graphite.

The electrodes fabricated using this process penetrate through the diamond bulk, and this "3D" geometry is shown in Figure 1. This contrasts with the planar geometry, where electrodes are fabricated on each side of the diamond bulk. The electrode separation is shorter in the 3D geometry compared to the planar geometry, which reduces the drift time of the charge carriers and lowers the trapping probability. This increases the detection efficiency, hence demonstrating the advantage of a 3D geometry.

The fabrication of graphitic electrodes uses a flat-incident wavefront, and the focal spot of the laser is distorted by refraction at the surface of the diamond. During the fabrication process, the aberrations of the beam change with the focal spot position, distorting the focal spot further. Using a spatial light modulator (SLM) in an established process [4], the laser focus is altered at different depths

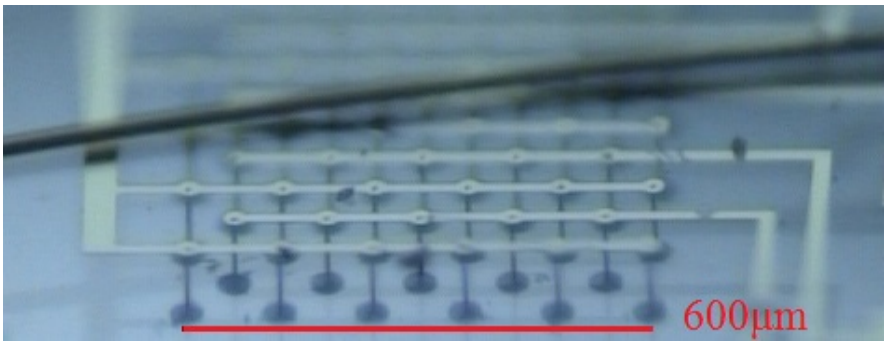

Figure 1: A 3D diamond detector produced in Manchester

in the diamond bulk by correcting for the aberration of the beam, and hence dynamically alters the wavefront of the laser. This results in a smaller focal spot with a higher energy density such that smaller electrodes may be fabricated.

3. Characterisation of electrodes

Graphitic electrodes were fabricated using a laser setup with an SLM and without an SLM, with average diameters of $\approx 1\,\mu m$ and $\approx 6\,\mu m$ respectively. The electrical properties of graphitic electrodes in diamond are assessed using Current-Voltage (IV) curves measured with a Keithley 2410 SourceMeter [5]. Both techniques produce ohmic electrodes, with a lower resistance observed when using an adaptive wavefront. This results in resistivities of $0.2\,\Omega cm$ and $2.5\,\Omega cm$ with and without an SLM, respectively.

The material content of the graphitic electrodes is determined via Raman spectroscopy using a HORIBA LabRAM HR Evolution Raman Spectrometer [6]. Typically three peaks are observed using this technique; a sharp, narrow peak at $1330\,cm^{-1}$ (corresponding to diamond), and two smaller, broader peaks at $1350\,cm^{-1}$ and $1583\,cm^{-1}$ (corresponding to graphite D ("disorganised") and graphite G ("organised") respectively) [7]. Fits are applied to the spectra to extract the heights of the diamond and graphite peaks (Figure 2), and the ratio of the diamond and graphite G peaks gives a measure of the graphite content inside the electrode. This ratio is lower $(0.2 - 0.4)$ when using an

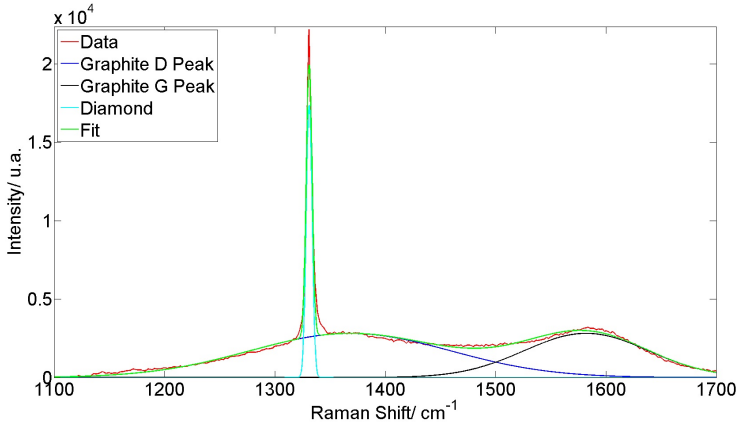

(a)

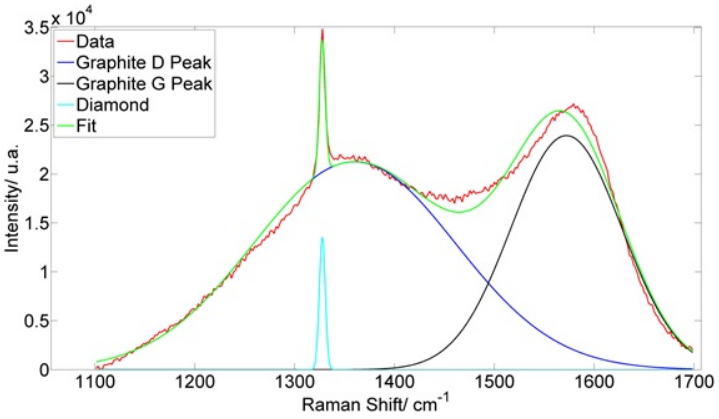

(b)

Figure 2: Raman spectra of electrodes produced without (a) and with (b) an SLM.

adaptive wavefront than without $(2-4)$. This is consistent with the resistivity measurements, where a lower ratio implies the electrodes have a higher content of graphite and hence greater electrode conductivity.

60 The degree of stress induced by graphitic electrodes in diamond is viewed using polarisers crossed at 90°. The bright areas signify high levels of stress within the diamond bulk. A comparison of cross polarised images for the two samples (Figure 3) shows the dominant source of stress without using an adaptive wavefront is from the electrodes on the diamond bulk. When using an

adaptive wavefront, the dominant source of stress is from the diamond sample itself. This implies the electrodes can be fabricated with a much smaller separation, lowering the charge collection distance. The lower stress also reduces the risk of damaging the diamond bulk and causing defects to neighbouring electrodes.

This technique is also used to determine the electrode yield. Electrodes with low surrounding stress indicate that electrode may be partially formed. The areas highlighted in Figure 3 show partially formed electrodes, which are confirmed using a microscope. Electrodes fabricated using an adaptive wavefront show a 100% yield, indicating that accounting for the aberrations of the beam is a reliable method for electrode fabrication.

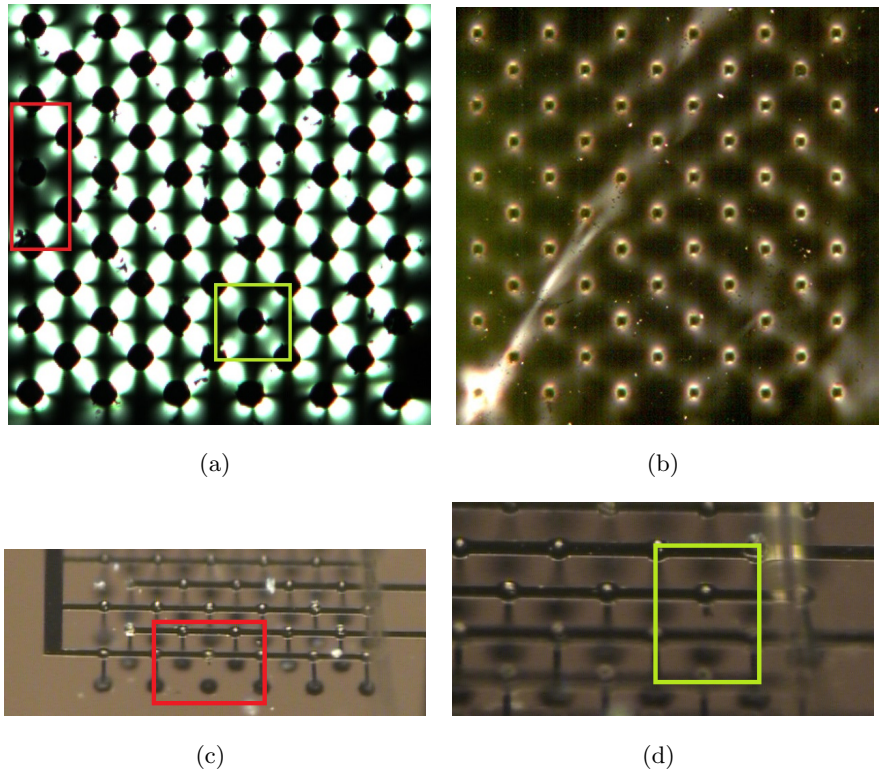

(a) (b)

(c) (d)

Figure 3: Cross polarised images of samples produced without (a) and with (b) an SLM. (c) and (d) Partially formed electrodes fabricated without an SLM.

4. Conclusions and outlook

Graphitic electrodes have been fabricated in diamond using a flat and a dynamically adaptive wavefront. A comparison of the techniques shows a reduction in the resistivity of the electrodes and the amount of induced stress by the electrodes using a dynamically adaptive wavefront, while increasing the graphitic content of the electrodes. The performance of 3D diamond detectors made using an dynamically adaptive wavefront will be investigated with particle beams and compared to a detector manufactured using a flat incident wavefront [8].

Acknowledgements

S. Murphy would like to acknowledge support from the Science and Technologies Facilities Council.

References

[1] C. Inc., Libra Series Data Sheet, http://www.coherent.com/downloads/LibraSeries_CoherentDataSheet_revC_May2013_4.pdf (2013).

[2] T. Kononenko et al., Femtosecond laser microstructuring in the bulk of diamond, Diamond and Related Materials 18 (2009) 196–199. doi:10.1016/j.diamond.2008.07.014.

[3] T. Kononenko et al., Microstructuring of diamond bulk by IR femtosecond laser pulses, Applied Physics A 90 (2008) 645–651. doi:10.1007/s00339-007-4350-9.

[4] B. Sun, P. Salter, M. Booth, High conductivity micro-wires in diamond following arbitrary paths, Applied Physics Letters 105. doi:10.1063/1.4902998.

[5] Textronix, Keithley Sourcemeter Data Sheet, http://www.keithley.com/products/software/?path=2410/Documents#4 (2015).

[6] H. Ltd., LabRAM HR Evolution Raman Spectrometer, http://www.horiba.com/uk/scientific/products/raman-spectroscopy/raman-spectrometers/raman-microscopes/hr-evolution/labram-hr-evolution-17309/ (2015).

[7] S. Reich, C. Thomsen, Raman spectroscopy of graphite, Royal Society Publishing 362 (2004) 2271–2288. doi:10.1098/rsta.2004.1454.

[8] G. Forcolin et al., Study of a 3D diamond detector with photon and proton micro-beams, Diamond and Related Materials 65 (2016) 75–82. doi:10.1016/j.diamond.2016.02.005.